Radiation Measurements 79 (2015) 33–42

Contents lists available at ScienceDirect

Radiation Measurements

journal homepage: www.elsevier.com/locate/radmeas

Bleaching of the post-IR IRSL signal from individual grains of K-feldspar: Implications for single-grain dating

R.K. Smedley*, G.A.T. Duller, H.M. Roberts

Department of Geography and Earth Sciences, Aberystwyth University, Ceredigion, SY23 3DB, UK

HIGHLIGHTS

- The bleaching rate of the pIRIR signal from single K-feldspar grains was assessed.
- The $pIRIR_{225}$ signal bleaches more rapidly than the $pIRIR_{290}$ signal.
- $pIRIR_{225}$ and $pIRIR_{290}$ signals reach the same level after 4–20 h of bleaching.
- The bleaching rate of the pIRIR signal varies from one grain to another.
- Variable pIRIR bleaching rates do not control single-grain D_e distributions.

ARTICLE INFO

Article history:
Received 12 June 2013
Received in revised form
18 May 2015
Accepted 5 June 2015
Available online 9 June 2015

Keywords:
Feldspar
Luminescence
Single grains
Infrared stimulated luminescence
pIRIR
Residual D_e values
Bleaching rate

ABSTRACT

Post-IR IRSL (pIRIR) signals from K-feldspar grains measured at elevated temperatures are increasingly being used for dating sediments. Unfortunately the pIRIR signal from K-feldspars bleaches more slowly than other signals (e.g. OSL from quartz) upon exposure to daylight, leading to concerns about residual signals remaining at deposition. However, earlier studies have not assessed whether the pIRIR signal bleaches at the same rate in all feldspar grains. In this study laboratory bleaching experiments have been conducted and for the first time the results show that the rate at which the pIRIR signal from individual K-feldspar grains bleach varies. To determine whether grain-to-grain variability in bleaching rate has a dominant control on equivalent dose (D_e) distributions determined using single grains, analysis was undertaken on three samples with independent age control from different depositional environments (two aeolian and one glaciofluvial). The D_e value determined from each grain was compared with the rate at which the $pIRIR_{225}$ signal from the grain bleaches. The bleaching rate of each grain was assessed by giving a 52 Gy dose and measuring the residual D_e after bleaching for an hour in a solar simulator. There is no clear relationship between the rate at which the $pIRIR_{225}$ signal of an individual grain bleaches and the magnitude of its D_e. It is concluded that variability in the bleaching rate of the $pIRIR_{225}$ signal from one grain to another does not appear to be a dominant control on single grain D_e distributions.

© 2015 The Authors. Published by Elsevier Ltd. This is an open access article under the CC BY license (http://creativecommons.org/licenses/by/4.0/).

1. Introduction

Optically stimulated luminescence (OSL) dating of single grains is beneficial in certain depositional environments (e.g. glaciofluvial settings) to detect the partial bleaching of sedimentary grains (Duller, 2008). A major challenge for single-grain measurements using quartz is that commonly only 5% or fewer of the grains emit a detectable OSL signal e.g. Duller (2006) detected as few as 0.5% of quartz grains in glaciofluvial sediments from Chile. In contrast to quartz, a larger proportion of K-feldspar grains are reported to emit a detectable OSL signal and the signals are also typically brighter (e.g. Duller et al., 2003). However, a major drawback for luminescence dating of feldspars is that the infrared stimulated luminescence signal measured at 50 °C (IR_{50}) is prone to anomalous fading over time, which some workers claim to be a ubiquitous phenomenon (e.g. Huntley and Lamothe, 2001). Currently there are two single aliquot regenerative dose (SAR) protocols commonly used for K-feldspar dating, (1) IR_{50} measurements, (e.g. Wallinga et al., 2000), and (2) post-IR IRSL measurements typically performed at 225 °C or 290 °C, giving rise to the $pIRIR_{225}$ and $pIRIR_{290}$ signals (e.g. Thomsen et al., 2008, 2011). Since the development of pIRIR measurement protocols, they have been

* Corresponding author.
E-mail address: rks09@aber.ac.uk (R.K. Smedley).

http://dx.doi.org/10.1016/j.radmeas.2015.06.003
1350-4487/© 2015 The Authors. Published by Elsevier Ltd. This is an open access article under the CC BY license (http://creativecommons.org/licenses/by/4.0/).

widely applied to coarse-grained K-feldspars (e.g. Buylaert et al., 2009, 2012) as the pIRIR signals are thought to access more distal donor-acceptor pairs than the IR_{50} signal and are therefore more stable over geological time, minimising the effects of anomalous fading on the pIRIR signal used for dating (Jain and Ankjærgaard, 2011).

Although the pIRIR signal may be more stable over time than the IR_{50} signal, several studies of coarse-grain K-feldspar using multiple grains have obtained bleaching curves which show that the pIRIR signal bleaches more slowly in response to optical stimulation than the IR_{50} signal (e.g. Buylaert et al., 2012, 2013; Kars et al., 2014; Murray et al., 2012), which in turn bleaches more slowly than the quartz OSL signal (Godfrey-Smith et al., 1988). More recently, Colarossi et al. (in press) have directly compared the bleaching rates using multiple grain measurements of feldspars and quartz, confirming previous findings, and showing that the $pIRIR_{290}$ signal bleaches more slowly than the $pIRIR_{225}$ signal. Equivalent dose (D_e) values for the pIRIR signal measured for modern analogues, or the residual D_e values remaining after laboratory bleaching of coarse-grained K-feldspar (Table 1) have been published for different pIRIR signals measured at different temperatures (e.g. Li et al., 2014). The smallest residual D_e values reported for multiple grains ($\leq$1 Gy) are measured using procedures with the lowest preheat and pIRIR stimulation temperatures (e.g. $pIRIR_{150}$ and $pIRIR_{180}$ protocols). It has therefore been suggested that lower temperature pIRIR protocols may be more appropriate for dating young sediments (e.g. Madsen et al., 2011; Reimann et al., 2011; Reimann and Tsukamoto, 2012). However, the model proposed by Jain and Ankjærgaard (2011) suggests that higher temperature pIRIR protocols access signals that are more stable over geological time. Thus, the $pIRIR_{225}$ and $pIRIR_{290}$ signals have the potential to provide more accurate and precise single-grain K-feldspar ages by further minimising the influence of fading beyond that of the pIRIR signals measured at lower temperatures.

Feldspars form a solid-solution series, ranging from anorthite ($CaAl_2Si_2O_8$), to albite ($NaAlSi_3O_8$), to orthoclase ($KAlSi_3O_8$). Density separation is routinely used for luminescence dating of sedimentary grains to isolate the K-feldspar fraction. However, geochemical measurements have demonstrated that density-separated K-feldspar fractions can be composed of different types of feldspar grains, which are chemically variable (e.g. Smedley et al., 2012). Thus far, bleaching curves have not been reported for single grains of K-feldspar. Investigating the grain-to-grain variability of bleaching rates of feldspars is important for single-grain dating as it has been suggested that the TL signal from different types of museum specimen feldspars bleaches at different rates in response to sunlight bleaching (e.g. Robertson et al., 1991). However, it has also been reported that the IRSL signal of different types of museum specimen feldspars bleaches at similar rates in response to a range of monochromatic wavelengths from 400 to 1065 nm (e.g. Spooner, 1994; Bailiff and Poolton, 1991). Thus, it is not clear whether the pIRIR signals from individual grains of K-feldspar in the density-separated fraction, composed of grains that have different internal K-contents, will bleach at different rates or not. The aim of this study is to investigate the bleaching of the $pIRIR_{225}$ and $pIRIR_{290}$ signals from single grains of K-feldspar and to examine whether any difference in bleaching rate may influence the D_e determined. Three samples of density-separated K-feldspars extracted from different depositional environments with independent age control are used for these investigations.

Table 1
A summary table of published pIRIR residual D_e values obtained for coarse-grained K-feldspar from multiple-grain aliquots in various studies, and one single-grain study (* Reimann et al., 2012).

Reference	Depositional environment	Bleaching method	Protocol	Residual
Reimann and Tsukamoto (2012)	Coastal	17 h SOL2 bleach	$pIRIR_{150}$	0.4 Gy
		1 week of daylight exposure	$pIRIR_{150}$	0.7 Gy
Madsen et al. (2011)	Beach	Modern analogue	$pIRIR_{150}$	0.05 ± 0.01 Gy to 2.66 ± 0.06 Gy
Reimann et al. (2011)	Coastal	4 h SOL2 bleach	$pIRIR_{180}$	~1 Gy
Reimann et al. (2012)*	Coastal	Modern analogue	$pIRIR_{180}$	0.6 ± 0.03 Gy
		4 h SOL2 bleach	$pIRIR_{180}$	0.9 ± 0.04 Gy
Thomsen et al. (2008)	Beach sand	Modern analogue	$pIRIR_{225}$	2 Gy
Buylaert et al. (2009)	Beach sand	Modern analogue	$pIRIR_{225}$	1.4 ± 0.1 Gy
Alappat et al. (2010)	Deltaic core	4 h SOL2 bleach	$pIRIR_{225}$	~3 Gy
Thiel et al. (2012)	Shallow marine	Modern analogue	$pIRIR_{290}$	~2 Gy
Buylaert et al. (2012)	Coastal	Modern analogue	$pIRIR_{290}$	5 ± 2 Gy
Reimann et al. (2011)	Coastal	4 h SOL2 bleach	$pIRIR_{290}$	6.4 ± 1.2 Gy
Alexanderson and Murray (2012)	Glaciofluvial	5 h SOL2 bleach[a]	$pIRIR_{290}$	12 ± 0.6 Gy

[a] In this experiment the distance of each aliquot from the SOL2 light source was ~40 cm.

2. Equipment and measurement protocols

All luminescence measurements were performed using a Risø TL/OSL DA-15 automated single-grain system equipped with an infrared laser (830 nm) fitted with an RG-780 filter (3 mm thick) to remove any shorter wavelengths (Bøtter-Jensen et al., 2003; Duller et al., 2003), and a blue detection filter pack containing a BG-39 (2 mm), a GG-400 (2 mm) and a Corning 7–59 (2.5 mm) filter placed in front of the photomultiplier tube. The inclusion of the GG-400 filter is to ensure removal of the thermally unstable UV emission centred on 290 nm seen during IR stimulation of feldspars (e.g. Balescu and Lamothe, 1992; Clarke and Rendell, 1997). The system was equipped with a $^{90}Sr/^{90}Y$ beta source delivering ~0.04 Gy/s.

Single aliquot regenerative dose (SAR) $pIRIR_{225}$ and $pIRIR_{290}$ protocols were used for dose-recovery and residual dose experiments (Table 2). A high temperature bleach was used at the end of each SAR cycle (step 9, Table 2) to remove any remaining charge arising from the test-dose and prevent charge transfer from the T_x

Table 2
Experimental details for the single aliquot regenerative dose (SAR) pIRIR dose-recovery and residual-dose experiments performed throughout this study. Note that the regenerative- and test-doses (shown in brackets) were smaller for the residual-dose experiments than those of the dose-recovery measurements.

Step	Treatment
1	Dose
2	Preheat 250 °C or 320 °C
3	SG IRSL 2 s at 60 °C
4	SG IRSL 2 s at 225 °C or 290 °C
5	Test dose (52 Gy or 4 Gy)
6	Preheat 250 °C or 320 °C
7	SG IRSL 2 s at 60 °C
8	SG IRSL 2 s at 225 °C or 290 °C
9	SG IRSL 3 s at 330 °C

measurement through to the subsequent L_x measurement which may affect the accuracy of the dose determinations. The IRSL signal was summed over the first 0.3 s of stimulation and the background calculated from the final 0.6 s. Regenerative doses of 0, 24, 48, 96 Gy and 0, 2, 4, 8, 20 and 40 Gy were used for dose-recovery and residual-dose experiments, respectively. A second 0 Gy dose was repeated after the largest regenerative dose as a second test for recuperation, which was then followed by a dose of 48 Gy (dose-recovery tests) or 8 Gy (residual-dose tests) used for recycling ratio tests.

Four rejection criteria were applied throughout the analyses unless otherwise specified; (1) whether the response to the test dose was less than three times the standard deviation of the background, (2) whether the uncertainty in the luminescence measurement of the test dose was greater than 10%, (3) whether the recycling ratio was outside the range 0.9–1.1, taking into account the uncertainties on the individual recycling ratios, and (4) whether recuperation was greater than 5% of the response from the largest regenerative doses, which were 96 Gy and 40 Gy for dose-recovery and residual dose experiments, respectively. Following the method of Thomsen et al. (2005) the instrument reproducibility of the single-grain measurement system was assessed for the protocols used in this study, giving values of 4.6% and 4.5% (per stimulation when the signal is summed over the initial 0.3 s) for the $pIRIR_{225}$ and $pIRIR_{290}$ measurements, respectively (Smedley and Duller, 2013). These instrument reproducibility values were incorporated into the D_e calculations.

3. Sample descriptions

Three samples of density-separated K-feldspar grains were used in this study. Sample TC01 was collected from an inland dunefield in eastern Argentina and has a multiple grain quartz OSL age (20 ± 5 years) indicating very recent deposition. Sample GDNZ13 was taken from a Late Glacial dune sand from North Island, New Zealand and is overlain by the Kawakawa tephra, which has been dated by radiocarbon to 25.36 ± 0.16 cal. ka BP (Vandergoes et al., 2013). Sample LBA12F4-2 was extracted from glaciofluvial sediments in Patagonia, directly linked to a moraine ridge dated to 25.2 ± 0.4 ka using cosmogenic isotope dating (^{10}Be) of moraine boulders (Kaplan et al., 2011).

Prior to measurement the samples were all treated with a 10% v.v. dilution of 37% HCl and with 20 vols H_2O_2 to remove carbonates and organics, respectively. Dry sieving isolated the 180–212 μm diameter grains, and density-separation with sodium polytungstate provided the <2.58 g cm^{-3} (K-feldspar-dominated) fractions. The K-feldspar grains were not etched in hydrofluoric acid because of concern about non-isotropic removal of the surface (Duller, 1992). Details of the calculation of the alpha dose-rates for these samples are described in the caption of Table 3. Finally, the K-feldspar grains were mounted into 10 × 10 grids of 300 μm diameter holes in a 9.8 mm diameter aluminium single-grain disc for analysis.

Dose-rates were calculated for the K-feldspar dominated fractions of all three samples using thick source alpha and beta counting on *Daybreak* and *Risø GM-25-5* measurement systems, respectively (Table 3). The K-content of each feldspar separate was measured using a Risø GM-25-5 beta counter to analyse 0.1 g subsamples of the separated material; this gave values of 6.5% K (TC01), 6.2% K (GDNZ13), and 3.9% K (LBA12F4-2). To calculate the internal dose rate arising from K within the feldspar grains a value of 10 ± 2% was used following the work of Smedley et al. (2012) and Smedley (2014) who showed that the K-content of the majority of grains from these samples which emitted detectable pIRIR signals was 10 ± 2%.

4. Determination of D_e remaining in a recently-deposited sample

The recently-deposited dune sand sample, TC01, was used to assess the residual D_e values for the $pIRIR_{225}$ and $pIRIR_{290}$ signals, using the protocols outlined in Table 2. Two hundred grains were measured using each signal but after applying the rejection criteria only 14 and 10 grains provided residual D_e values for the $pIRIR_{225}$ and $pIRIR_{290}$ signals, respectively. These single-grain residual D_e values are presented as histograms to show the populations of grains measured using the $pIRIR_{225}$ (Fig. 1a) and $pIRIR_{290}$ (Fig. 1b) signals. Although there was variation between the residual D_e values measured for individual grains, 12 of the 14 grains (86%) measured using the $pIRIR_{225}$ protocol and 6 of the 10 grains (60%) measured using the $pIRIR_{290}$ protocol gave residual D_e values of ≤2 Gy. The central age model (CAM) D_e values were calculated from the $pIRIR_{225}$ and $pIRIR_{290}$ single-grain populations, giving values of 1.0 ± 0.3 Gy and 1.7 ± 0.4 Gy, respectively.

Multiple-grain dating using the OSL signal from quartz gave a luminescence age for sample TC01 of 20 ± 5 years. For comparison, luminescence ages determined from single grains were also calculated using the CAM D_e values of the $pIRIR_{225}$ (CAM D_e value of 1.0 ± 0.3 Gy) and $pIRIR_{290}$ (CAM D_e value of 1.7 ± 0.4 Gy) signals, and the dose-rate in Table 3. The ages calculated for sample TC01 using the $pIRIR_{225}$ and $pIRIR_{290}$ signals for single-grains of K-feldspar were 325 ± 100 years and 550 ± 130 years, respectively.

The CAM D_e value calculated for the $pIRIR_{225}$ signal from the recently-deposited dune-sand sample (1.0 ± 0.3 Gy) is comparable to the published residual D_e values of <1 Gy for other samples using the $pIRIR_{180}$ signal shown in Table 1. However, the CAM D_e value (1.7 ± 0.4 Gy) calculated in this study using the $pIRIR_{290}$ signal was larger than 1 Gy. When a synthetic aliquot is derived by summing the signal emitted from all the grains on the single-grain disc, the mean D_e values calculated from two synthetic aliquots per signal were 1.4 Gy ($pIRIR_{225}$ signal) and 2.6 Gy ($pIRIR_{290}$ signal). These D_e values are consistent with the smallest residual dose values published for the pIRIR signals from multiple-grain aliquots of K-feldspar (Table 1), but slightly larger than the values derived from measurements using single grains.

Table 3
Dose-rates calculated for the density-separated K-feldspar fractions of the samples used in this study. Water contents are expressed as a percentage of the mass of dry sediment and were based on measurements of the field water contents and saturated water contents. An internal K-content of 10 ± 2% was applied for the K-feldspar fraction after Smedley et al. (2012). External dose-rates were determined using thick source alpha and beta counting. Dose-rates were calculated using the updated conversion factors of Guerin et al. (2011). An a-value of 0.11 ± 0.03 was used after measurements performed by Balescu and Lamothe (1993). Alpha and beta dose-rates were attenuated for grain size after Bell (1980) and Guerin et al. (2012), respectively. Attenuation for moisture content was calculated after Zimmerman (1971). The cosmic dose-rate was calculated based on Prescott and Hutton (1994).

Sample	Grain size (μm)	Water content (%)	K (%)	U (ppm)	Th (ppm)	Cosmic dose-rate (Gy/ka)	Dose-rate (Gy/ka)
TC01	180–250	5 ± 2	1.72 ± 0.08	1.89 ± 0.19	4.38 ± 0.61	0.18 ± 0.02	3.08 ± 0.17
GDNZ13	180–212	30 ± 5	1.02 ± 0.07	2.26 ± 0.19	5.25 ± 0.61	0.14 ± 0.02	2.23 ± 0.14
LBA12F4-2	180–212	5 ± 2	2.35 ± 0.11	1.99 ± 0.24	6.37 ± 0.80	0.09 ± 0.02	3.75 ± 0.46

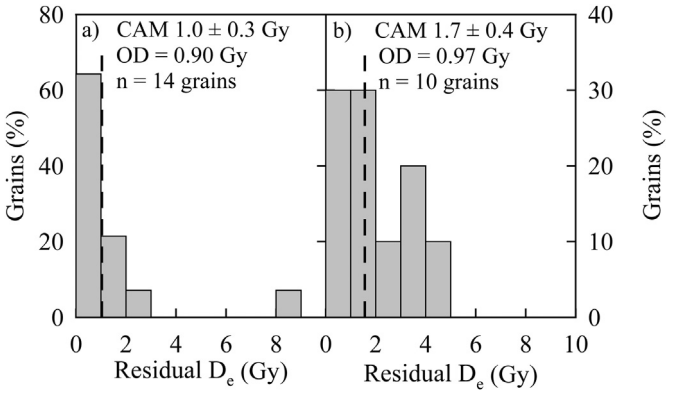

Fig. 1. Histograms of the single-grain population of natural D_e values obtained for the recently-deposited sample TC01 using the $pIRIR_{225}$ (a) and $pIRIR_{290}$ (b) signal. The dashed line marks the central age model (CAM) D_e value calculated for the single-grain population.

Dose-recovery experiments were performed on a suite of 200 fresh grains from sample TC01 using both the $pIRIR_{225}$ and $pIRIR_{290}$ signals to assess the suitability of each measurement protocol. A 52 Gy dose was added to the small natural dose as measured above and the resultant D_e was assessed using the pIRIR protocols outlined in Table 2. The CAM D_e for the $pIRIR_{225}$ and $pIRIR_{290}$ signals gave residual-subtracted dose-recovery ratios of 0.98 ± 0.02 and 0.97 ± 0.04, and overdispersion values of 9.6 ± 0.4% (n = 37 grains) and 17.9 ± 0.4% (n = 45 grains), respectively, demonstrating the appropriateness of both of these protocols for determining D_e values.

5. Measurement of D_e remaining after laboratory bleaching

The measurements from the naturally-bleached sample, TC01 (Section 4), demonstrate the degree of variation in residual D_e values expected in a well-bleached environment. However, single-grain dating is typically used to analyse sediments in environments where the opportunities for bleaching are limited (Duller, 2008). Thus, an investigation of the residual D_e values observed in response to different bleaching times was conducted to assess the grain-to-grain variability in the rate of bleaching of the pIRIR signal.

5.1. Experimental design

Eight hundred grains that had previously been analysed to determine the natural D_e value (400 grains from sample TC01, and 400 grains from sample GDNZ13) were used for these experiments to assess the residual D_e values measured following different laboratory bleaching durations. For each sample, half of the 400 grains were measured using a $pIRIR_{225}$ protocol, and the other half were measured using the $pIRIR_{290}$ protocol. Prior to these measurements, the grains were given a 52 Gy dose and then bleached at a distance of ~50 cm from the bulb of a SOL2 solar simulator for different periods of time. L_x/T_x measurements were performed after each bleaching interval and interpolated on to a dose-response curve previously constructed for each individual grain. Replicate measurements were performed on the same grains after different intervals of 1, 4, 8, and 20 h to monitor the depletion of the pIRIR signals for individual grains.

5.2. Laboratory bleaching of an Argentinean dune sand

The CAM was applied to residual D_e values obtained from single grains of TC01 which passed the rejection criteria (Section 2) for the $pIRIR_{225}$ (Fig. 2, closed diamonds; n = 15 grains) and $pIRIR_{290}$ (Fig. 2, open circles; n = 19 grains) signal, measured after the different laboratory bleaching times. The $pIRIR_{225}$ and $pIRIR_{290}$ CAM D_e values determined for the naturally-bleached grains of TC01 (Section 4) are also marked as dashed lines in Fig. 2 for comparison. Neither the $pIRIR_{290}$ nor the $pIRIR_{225}$ signal deplete to the natural residual D_e value, even after a prolonged 20 h bleach in the SOL2, which is equivalent to ~5 ½ days of natural sunlight exposure. Instead, the $pIRIR_{225}$ and $pIRIR_{290}$ CAM D_e values reduced to only 5.0% and 6.6% of the 52 Gy given doses, respectively. The $pIRIR_{225}$ signal is shown in Fig. 2 to bleach more rapidly after 1 h of bleaching (5.6 ± 0.8 Gy residual D_e; 11% of the given dose) than the $pIRIR_{290}$ signal (9.2 ± 1.0 Gy residual D_e; 18% of the given dose). However, beyond 4 h of bleaching, the residual D_e values for both signals are similar to one another, and after 20 h both the $pIRIR_{225}$ and $pIRIR_{290}$ signals gave a CAM D_e value ~5% of the 52 Gy given dose.

The bleaching rate of the $pIRIR_{225}$ signal from single grains of sample TC01 is shown in Fig. 3, and demonstrates that different grains bleach at different rates. Three grains that bleach at different rates (fast, moderate, slow) are highlighted in Fig. 3a (denoted grains a, b and c). Grain (a) bleaches rapidly to a residual D_e value of 2.4 ± 1.0 Gy (4.6% of the given dose) after 1 h of bleaching and remains at ~2 Gy for the prolonged bleaching times. Grain (b) has a moderate bleaching rate, reaching a residual D_e value of 7.6 ± 0.8 Gy (15% of the given dose) after 1 h of bleaching and reduces to a value of 2.1 ± 0.3 Gy (4.1% of the given dose) after the prolonged 20 h bleach. Grain (c) bleaches the slowest, giving a residual D_e value of 15.4 ± 2.0 Gy (29.6% of the given dose) after 1 h of bleaching with a

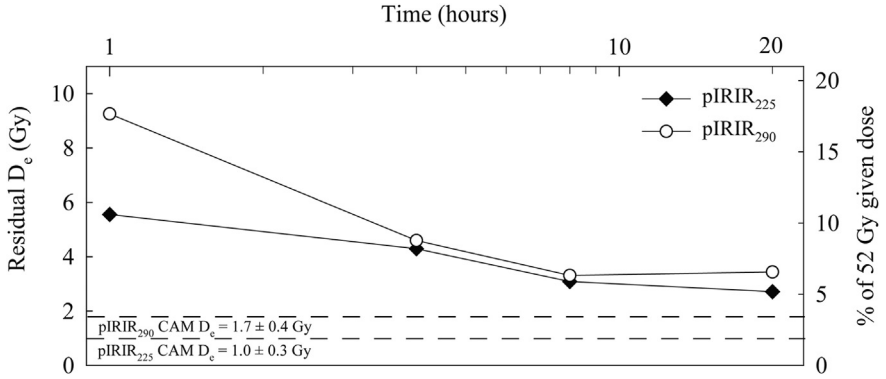

Fig. 2. Central age model (CAM) residual D_e values calculated from the single-grain population of TC01 after a 52 Gy given dose followed by SOL2 bleaching intervals of 1, 4, 8 and 20 h. Data are presented for the $pIRIR_{225}$ and $pIRIR_{290}$ signals. The horizontal dashed lines mark the CAM D_e values calculated from the naturally-bleached grains from Fig. 1.

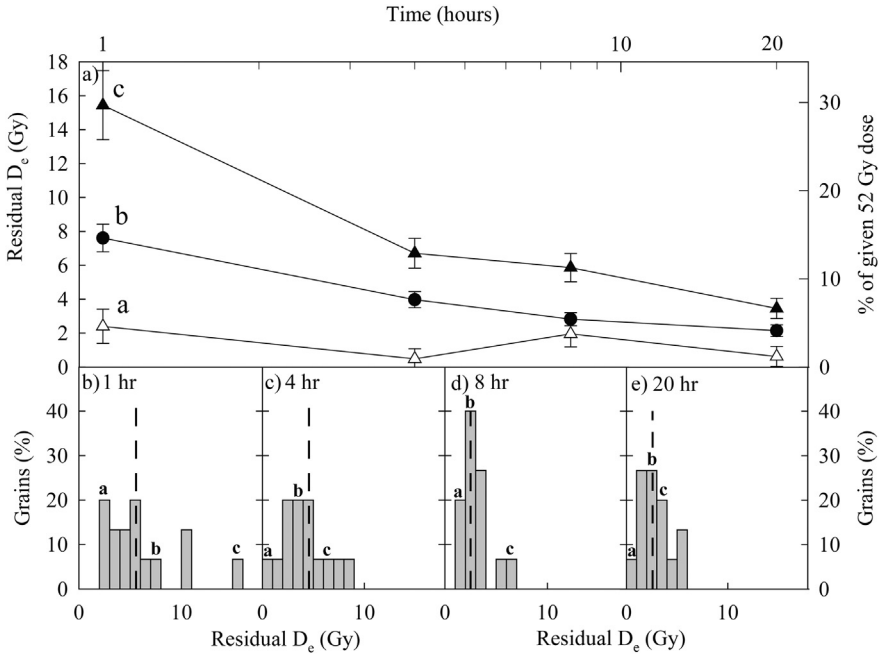

Fig. 3. Grain-to-grain variability in residual D_e values obtained for sample TC01 using the $pIRIR_{225}$ signal. a) Examples of individual grains that have a rapid (a; open triangles), moderate (b; closed circles) and slow (c; closed triangles) bleaching rate. Histograms are also presented showing the single-grain population of D_e values following exposure to the SOL2 for (b) 1, (c) 4, (d) 8 and (e) 20 h. Residual D_e values of grains a, b and c within the single-grain populations are indicated. The CAM residual D_e value calculated from the grains of each histogram is represented by the vertical dashed line in Figs b–e.

SOL2 but reaches a value of 3.5 ± 0.6 Gy (6.6% of the given dose) after a 20 h bleach. Although the bleaching rates of individual grains varies, all three of the grains (a, b and c) have residual D_e values of ≤10% of the given dose after 20 h of bleaching. The implication of this is that for samples from environments where grains are exposed to long periods of sunlight, the variability in residual D_e value from one grain to another at deposition will be small, and hence would be expected to contribute little to scatter in D_e distributions determined from single grains. Whilst the variability in D_e from one grain to another may be small, the average residual D_e remaining even after 20 h in the SOL2 (Fig 3e) is 2.7 ± 0.3 Gy, which would be significant when dating young samples.

The residual D_e values of grains (a), (b) and (c) relative to the rest of the single-grain population are also shown as histograms in Fig. 3, representing the different bleaching times used, namely 1 h (Fig. 3b), 4 h (Fig. 3c), 8 h (Fig. 3d) and 20 h (Fig. 3e). The single-grain population has a large range of residual D_e values after the shorter, 1 h bleach (2–15.5 Gy) and a smaller range in residual D_e values after the 20 h bleach (0–5.5 Gy). Moreover, there is an identifiable population of grains that bleach more rapidly (e.g. grain a). After a short 1 h bleach ~20% and ~50% of the grains bleach to ≤5% and ≤10% of the given dose, respectively. The grain-to-grain variability of bleaching of the pIRIR signal demonstrates that a population of grains (e.g. grain a) bleaches more rapidly in response to optical stimulation than others (e.g. grains b and c); these rapidly-bleaching grains may be preferable for single-grain analysis of the pIRIR signal from partially-bleached sediments as they might be expected to have the smallest residual D_e values upon deposition.

5.3. Laboratory bleaching of a New Zealand dune sand

The same experiment as that discussed in Sections 5.1 and 5.2 was undertaken for the Late Glacial dune sand sample from New Zealand, GDNZ13. The CAM D_e values calculated from the single-grain populations of sample GDNZ13 measured after the different SOL2 bleaching times are presented in Fig. 4a for the $pIRIR_{225}$ (n = 45 accepted grains; closed diamonds) and $pIRIR_{290}$ (n = 38 accepted grains; open circles) signals. The CAM $pIRIR_{225}$ D_e of GDNZ13 is 6.5 ± 0.5 Gy (12.6% of the given dose) after 1 h and 3.7 ± 0.3 Gy (7.1% of the given dose) after 20 h of bleaching (Fig. 4a). However, the $pIRIR_{290}$ signal of GDNZ13 bleaches comparatively slowly giving a residual D_e value of 12.4 ± 1.1 Gy (23.8% of the given dose) after 1 h and 5.3 ± 0.5 Gy (10.2% of the given dose) after 20 h in the SOL2.

The distribution of D_e values for individual grains of sample GDNZ13 measured using the $pIRIR_{225}$ signal was similar to that seen for sample TC01 in Fig. 3 (b–d). Histograms of the residual D_e values of the single-grain population measured for GDNZ13 are presented in Fig. 4 for 1 h (Fig. 4b), h (Fig. 4c), 8 h (Fig. 4d) and 20 h (Fig. 4e) bleaching with the SOL2; highlighted on each graph is the CAM D_e value calculated for each bleaching time (dashed line). Although the data are not shown here, the grain-to-grain variability in bleaching was larger for the $pIRIR_{290}$ signal in comparison to the $pIRIR_{225}$ signal for this sample. No grains bleached to residual levels ≤5% of the given dose after a 1 h SOL2 bleach using the $pIRIR_{290}$ signal for GDNZ13, however, 11% of the grains did bleach to ≤10% of the given dose after a 1 h bleach. The $pIRIR_{225}$ and $pIRIR_{290}$ data from GDNZ13 and TC01 demonstrates that different grains bleach at different rates.

5.4. Dependence of residual D_e on prior dose

Sohbati et al. (2012) measured the dose-dependence of $pIRIR_{225}$ residual D_e values using multiple-grain aliquots of K-feldspar for samples from southeast Spain. Larger residual D_e values were obtained following a 4 h SOL2 bleach for the samples with the larger natural D_e values (up to ~1000 Gy). The dataset was extrapolated to derive an estimate for the residual D_e value at deposition of

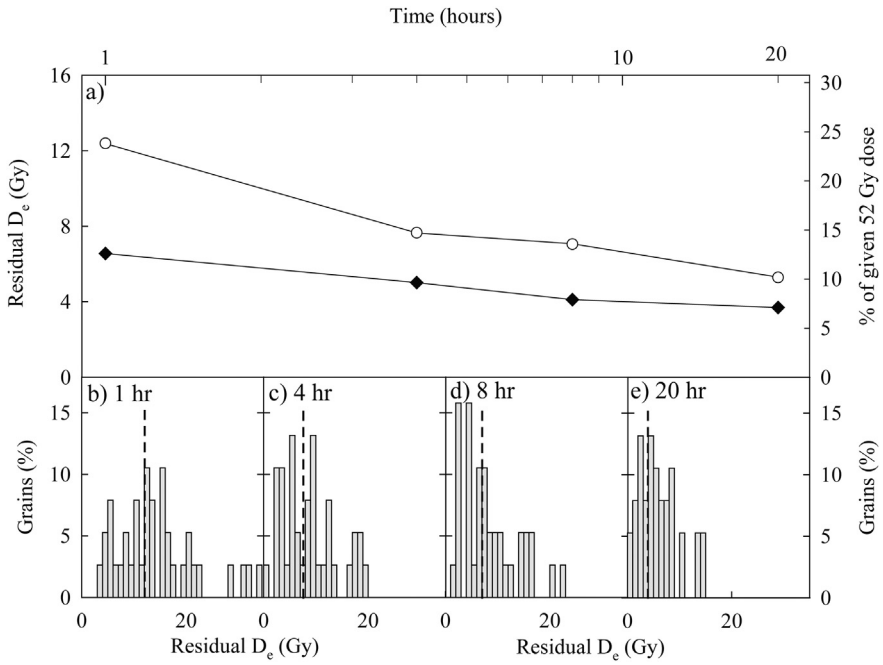

Fig. 4. Central age model (CAM) residual D_e values calculated from the single-grain population of GDNZ13 after SOL2 bleaching of 1, 4, 8 and 20 h a) Data are presented for the $pIRIR_{225}$ and $pIRIR_{290}$ signal. Histograms of single-grain residual D_e values obtained for the $pIRIR_{225}$ signal after SOL2 bleaching intervals of (b) 1, (c) 4, (d) 8 and (d) 20 h. The CAM D_e values calculated from the grains of each histogram are represented by the vertical dashed line in Figs b–e.

0.98 ± 0.8 Gy, which is similar to the residual D_e value determined for the recently-deposited aeolian dune sand sample, TC01, in this study (Section 4). In the current study, the impact of prior dose on the residual D_e of individual grains was assessed using given doses of different magnitudes prior to bleaching. One hundred grains of sample GDNZ13 that had been previously analysed to determine a natural D_e value (similar to the grains in Sections 5.2 and 5.3) were given a 52 Gy beta dose, bleached for 8 h in the SOL2 and the L_x/T_x ratios were measured. This procedure was repeated twice more following given doses of 102 Gy and 202 Gy, and the L_x/T_x values were interpolated on to a dose-response curve constructed for each individual grain to determine the residual D_e values.

The residual D_e values obtained for the $pIRIR_{225}$ signal of sample GDNZ13 are shown in Fig. 5a as a function of the given dose (i.e. 52 Gy, 102 Gy and 202 Gy). The CAM residual D_e value (Fig 5b–d, dashed lines) increased with increased given dose prior to bleaching in the SOL2, and is comparable to the residual D_e values measured by Sohbati et al. (2012). In the present study, the residual D_e values after different given doses for grains characterised by a fast, moderate or slow bleaching are highlighted in Fig. 5a (denoted grains x, y and z) for the $pIRIR_{225}$ signal of sample GDNZ13. Fig 5a shows that all three of the grains (x, y and z) give larger residual D_e values with larger given doses prior to bleaching. In the natural environment the dose each grain has received prior to the event being dated is unknown and so any variability in the rate at which the $pIRIR_{225}$ signal of the different grains bleaches can further complicate single-grain dose-distributions.

6. Grain-to-grain variability in bleaching rates of the pIRIR signal

Thus far, this study has demonstrated that the pIRIR signal of individual grains of K-feldspar have the potential to bleach at different rates in response to light. Previous studies have suggested that slow bleaching rates of the pIRIR signal may restrict the use of the pIRIR signal for dating of K-feldspar in partially-bleached environments (e.g. Blombin et al., 2012; Trauerstein et al., 2012). However, the influence that grain-to-grain variability in bleaching rates of the pIRIR signal has on single-grain D_e distributions has not yet been investigated for natural sedimentary samples.

The observation that the pIRIR signal of different grains bleaches at different rates suggests that dating of partially-bleached sediments may be optimised by trying to preferentially select for analysis those grains that bleach most rapidly. To test this idea, the bleaching rates of individual grains of K-feldspar were assessed by measuring the residual D_e values after a short 1 h bleach in order to force the largest divergence in behaviour between the more- and less-rapidly bleaching grains in the dataset (e.g. Fig. 3b). These short laboratory bleaching tests involved (1) a given dose of 52 Gy, followed by (2) a 1 h bleach in the SOL2 solar simulator, and (3) single-grain L_x/T_x measurements, which are then interpolated on to the original dose-response curves constructed for dating. The residual D_e values measured during these bleaching tests give an indication of the relative bleaching rates of the individual grains that form the single-grain D_e distribution.

Short bleaching tests were performed using the $pIRIR_{225}$ and $pIRIR_{290}$ signals on a further suite of single grains of K-feldspar extracted from sample GDNZ13. The single-grain data were first ranked from the smallest to the largest by the residual D_e values, and then the cumulative percentage of grains (y-axis) were plotted against the residual D_e values as a percentage of the 52 Gy given dose (x-axis). Fig. 6a compares the bleaching rates measured for sample GDNZ13 using the $pIRIR_{225}$ and $pIRIR_{290}$ signals. There was more variability in the single-grain residual D_e values measured after a 1 h SOL2 bleach using the $pIRIR_{290}$ signal in comparison to the $pIRIR_{225}$ signal; ~80% of the grains reduced to residual D_e values that were ≤31% of the given dose (i.e. ≤17 Gy) for the $pIRIR_{290}$ signal whilst for the $pIRIR_{225}$ signal the same proportion of grains had residual D_e values of ≤19% of the given dose (i.e. ≤10 Gy). This reinforces the view that the $pIRIR_{290}$ signal bleaches slower than the $pIRIR_{225}$ signal and this is reflected by the larger and more variable single-grain residual D_e values.

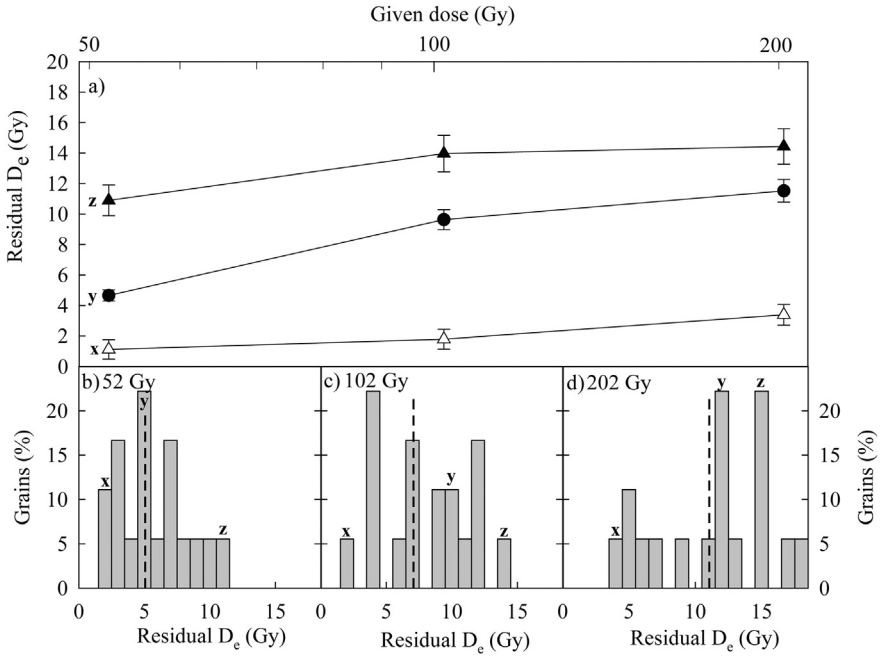

Fig. 5. Grain-to-grain variability in residual D_e values obtained using the $pIRIR_{225}$ signal for sample GDNZ13 after 8 h exposure to the SOL2. a) Examples of individual grains that have a rapid (x; open triangles), moderate (y; closed circles) and slow (z; closed triangles) bleaching rate. Note that the x-axis shows the given dose on a log scale. Histograms are also presented showing the single-grain population following given doses of (b) 52 Gy, (c) 102 Gy and (d) 202 Gy; residual D_e values of grains x, y and z within the single-grain population are indicated. The CAM residual D_e value calculated from the grains of each histogram is represented by the dashed line in Figs b–e.

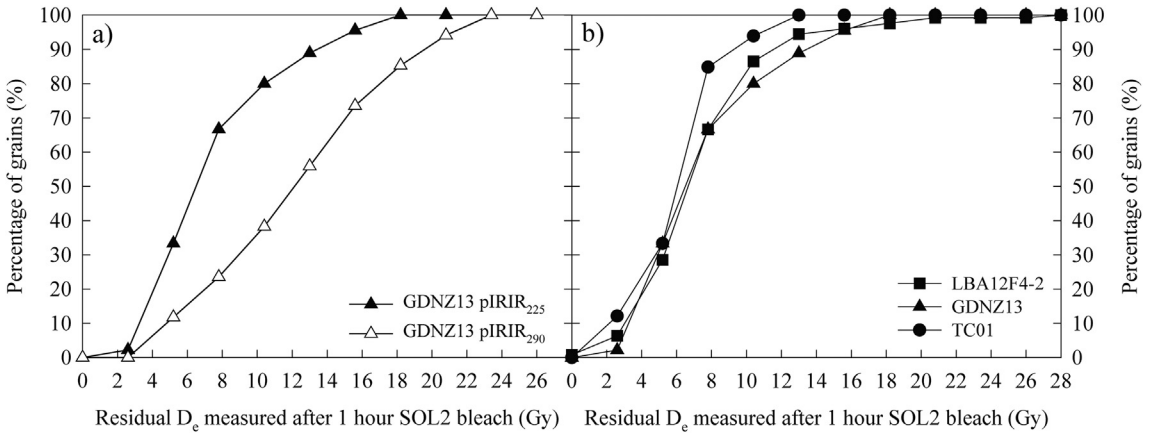

Fig. 6. Cumulative percentage of grains with residual D_e values expressed as a percentage of the 52 Gy given dose after a short 1 h SOL2 bleach. The single-grain data presented in this plot were ranked from the smallest to the largest by the residual D_e value, and the cumulative percentages of grains (y-axis) were then plotted against the residual dose as a percentage of the 52 Gy given dose (x-axis). Data are presented to compare (a) the $pIRIR_{225}$ and $pIRIR_{290}$ signals of sample GDNZ13 and (b) the $pIRIR_{225}$ signals of samples TC01, GDNZ13 and LBA12F4-2.

To assess whether the grain-to-grain variability in bleaching rate of the $pIRIR_{225}$ signal is a dominant control on the single-grain D_e distributions, the residual D_e values for the $pIRIR_{225}$ signal after the 1 h bleach in the SOL2 solar simulator were compared to the single-grain D_e values for three sedimentary samples from different depositional environments. The three samples tested were from different depositional settings and are constrained by independent age control (Section 3). Sample TC01 is a recently-deposited aeolian dune sand, sample GDNZ13 is a Late Glacial aeolian sand, and sample LBA12F4-2 is a glaciofluvial sample deposited during the Last Glacial period. The short laboratory bleaching tests were performed for all three samples after the measurement of the $pIRIR_{225}$ signal to determine the natural D_e values. Fig. 6b compares the bleaching rates measured for the three different samples and demonstrates that there was little difference between the samples in the behaviour of the $pIRIR_{225}$ signal. After the 1 h bleach in the SOL2 solar simulator, the typical behaviour shown by all three samples is that the measured D_e values of ~80% of all the grains reduced to ≤20% of the given dose (i.e. ≤10.4 Gy) (Fig. 6b). The bleaching tests and the D_e values were assessed using exactly the same grains to permit direct comparison between the inferred bleaching rates and the natural D_e values (Fig. 7). If bleaching rates were a dominant control on the single-grain D_e distribution then there would be a relationship between the residual D_e values measured after the short laboratory bleaching tests and the natural D_e values. The results in Fig. 7 for samples TC01 (a), GDNZ13 (c), and LBA12F4-2 (e) shows that there is no direct relationship between the inferred bleaching rates and the D_e values for single grains from

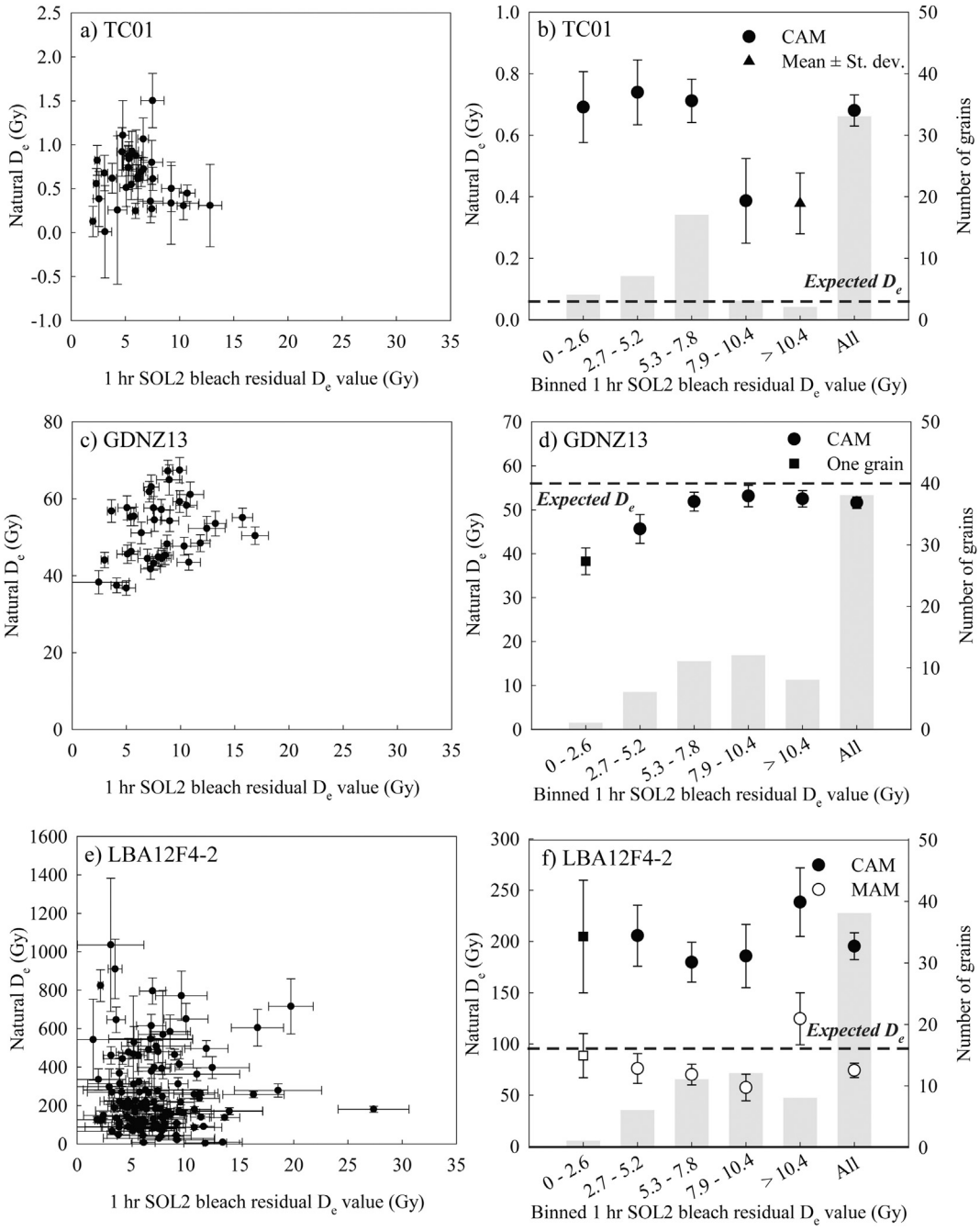

Fig. 7. Comparisons of the residual D_e value, measured in the laboratory after a 1 h bleach following a 52 Gy given dose, with the natural D_e value. All data were measured using the $pIRIR_{225}$ signal and are shown for samples TC01 (a), GDNZ13 (c) and LBA12F4-2 (e). The grains in (a), (c) and (e) were then ranked according to the size of the residual D_e measured after the 1 h SOL2 bleach following the 52 Gy given dose, and binned into five groups. The CAM and/or MAM D_e values for each bin were then calculated and plotted (b, d, f). For the MAM analysis a σ_b value of 0.3 was used. The D_e value expected for these samples is calculated from the dose-rate and independent age control. Fading tests of the $pIRIR_{225}$ signal were undertaken for samples GDNZ13 (g-value 3.5 ± 0.7%/decade, n = 5) and LBA12F4-2 (g-value 2.1 ± 1.3%/decade, n = 5) using multiple grain aliquots. The data presented here have not been corrected for fading because it is the pattern of relative change in D_e for grains with different bleaching rates that is primarily of interest. The number of grains used to calculate each D_e value is shown in the histograms (b, d and f). Where bins contained fewer than three grains, the mean and standard deviation D_e values were calculated for comparison.

any of the three samples.

The individual grains included in Fig. 7 were also ranked from smallest to largest according to the size of the residual D_e value measured after the short 1 h bleaching tests and binned into five groups (0–2.6 Gy, 2.7–5.2 Gy, 5.3–7.8 Gy, 7.9–10.4 Gy and >10.4 Gy). The number of grains included in each bin is shown in the histograms in Fig. 7 (b, d, f). The CAM D_e value was calculated for each bin of all three samples (Fig. 7b, d and f). MAM D_e values were also calculated for each bin of the glaciofluvial sample LBA12F4-2 (Fig. 7f) as the large overdispersion value calculated for single-grain D_e values of this sample (71.6 ± 0.1%; n = 260 grains) suggested that it was partially bleached upon deposition. Since these samples have independent age control, expected D_e values could be calculated using the dose-rates (Table 3). The CAM and/or

MAM D_e values calculated for all the grains of each sample are plotted in Fig 7 (b, d, f), in addition to the expected D_e value for each sample (Table 3).

If bleaching rates are a dominant control on the single-grain D_e distributions then the bins containing the grains with the $pIRIR_{225}$ signals that bleach most rapidly in response to exposure to the SOL2 solar simulator should give rise to the lowest CAM and MAM natural D_e values. For sample TC01 (Fig. 7b) the CAM D_e values calculated using the grains with the most rapidly-bleaching $pIRIR_{225}$ signal (230 ± 30 years) do not give ages in agreement with the OSL age obtained from quartz (20 ± 5 years). The results for sample GDNZ13 (Fig. 7d) show lower CAM natural D_e values for the binned grains that gave the lowest residual D_e values, but the bin representing residual D_e values of 0–2.6 Gy contains only one grain, and the difference between the CAM D_e value calculated for the 2.7–5.2 Gy bin and the bins >5.2 Gy is small.

The opportunity for bleaching in the natural environment is likely to be less in a glaciofluvial setting in comparison to an aeolian setting, and so differences in bleaching behaviour of individual grains (e.g. Fig. 3e) is likely to have a larger influence in a glaciofluvial setting. Fig. 7f presents the CAM and MAM natural D_e values calculated for the bins of grains for the glaciofluvial sample LBA12F4-2. The results show no trend between the CAM or MAM D_e values and the inferred bleaching rate of the grains. It is concluded that although differences are observed in the inferred bleaching rates of the $pIRIR_{225}$ signals of single grains, these variable bleaching rates are not a dominant control on the single-grain D_e distribution of these samples. Note that the bleaching rates of individual grains are not related to the extent of bleaching in the natural environment and so the two factors will likely impact samples taken from different depositional settings to different extents. Presumably for samples from well-bleached settings (e.g. aeolian) where the opportunity for resetting of the pIRIR signal is high, other factors such as internal geochemistry (K, Rb, U or Th), external microdosimetry and anomalous fading are a more dominant control on single-grain D_e distributions. This is in contrast to environments where the opportunity for bleaching is low (e.g. glaciofluvial or fluvial) and the extent of bleaching in the natural environment is the dominant control on the D_e distribution; this highlights why single-grain analysis is important for providing accurate ages for sedimentary samples taken from poorly-bleached settings.

7. Conclusions

A naturally-bleached dune sand from Argentina (TC01) that gave an age of 20 ± 5 years using the OSL signal of quartz, gave ages of 325 ± 100 years and 550 ± 130 years using single-grain measurements of the $pIRIR_{225}$ and $pIRIR_{290}$ signals, respectively. Laboratory measurements of residual D_e values after bleaching in a solar simulator were then used to investigate the variability in bleaching rates of the $pIRIR_{225}$ and $pIRIR_{290}$ signals for individual grains of K-feldspar from two aeolian dune samples (TC01 and GDNZ13). These bleaching experiments demonstrated that some grains bleach more rapidly than others in response to laboratory bleaching, regardless of the prior dose.

Although the pIRIR signals from individual grains bleach at variable rates, this variation appears to have little impact upon the natural D_e values determined for K-feldspar grains from the samples measured in this study (Fig 7). For the two aeolian samples it is likely that prior to deposition the grains experienced prolonged periods of sunlight bleaching and so all the grains, regardless of the potential rate of bleaching, reached low residual D_e values (c.f. 20 h bleach in Fig. 3a). The extended exposure to sunlight in an aeolian environment reduces the impact of variable bleaching rates on the natural D_e distributions (e.g. Fig. 7b, d). In contrast, the probability that individual grains have experienced prolonged periods of sunlight exposure in a glaciofluvial setting is low. It is likely that some grains experienced shorter exposure to sunlight than other grains and that the difference in bleaching rates would result in variable residuals in natural D_e distributions (e.g. Fig. 3a). However, the glaciofluvial sample shown in this study suggests that the influence that the bleaching rates of individual grains had on the natural D_e distributions (Fig. 7f) was minimal in comparison to other factors, including the variation due to the stochastic nature of the exposure of individual grains to sunlight.

The pIRIR signal from individual grains of K-feldspar bleaches at different rates, but analysis of the samples described here suggests that these differences in rate are not sufficiently great to have any discernible impact upon the D_e distribution obtained using single grains.

Acknowledgements

Financial support for the laboratory work contributing towards this paper was provided by a NERC PhD Studentship to RKS (NE/I1527845/1). Prof. Joanne Bullard (Loughborough University) is thanked for collecting the aeolian dune sand from Argentina (TC01). Aberystwyth Luminescence Research Laboratory (ALRL) benefits from being part of the Climate Change Consortium for Wales (C3W). Two anonymous reviewers are thanked for their comments that helped to improve the manuscript.

References

Alappat, L., Tsukamoto, S., Singh, P., Srikanth, D., Ramesh, R., Frechen, M., 2010. Chronology of Cauvery delta sediments from shallow subsurface cores using elevated-temperature post-IR IRSL dating of feldspar. Geochronometria 37, 37–47.

Alexanderson, H., Murray, A.S., 2012. Luminescence signals from modern sediments in a glaciated bay, NW Svalbard. Quat. Geochronol. 10, 250–256.

Bailiff, I.K., Poolton, N.R.J., 1991. Studies of charge transfer mechanisms in feldspars. Nucl. Tracks Radiat. Meas. 18, 111–118.

Balescu, S., Lamothe, M., 1992. The blue emission of K-feldspar coarse grains and its potential for overcoming TL age underestimation. Quat. Sci. Rev. 11, 45–51.

Balescu, S., Lamothe, M., 1993. Thermoluminescence dating of the Holsteinian marine formation of Herzeele, northern France. J. Quat. Sci. 8, 117–124.

Bell, W.T., 1980. Alpha dose attenuation in quartz grains for thermoluminescence dating. Anc. TL 12, 4–8.

Blombin, R., Murray, A., Thomsen, K.J., Buylaert, J.-P., Sobhati, R., Jansson, K.N., Alexanderson, H., 2012. Timing of the deglaciation in southern Patagonia: testing the applicability of K-feldspar IRSL. Quat. Geochronol. 10, 264–272.

Bøtter-Jensen, L., Andersen, C.E., Duller, G.A.T., Murray, A.S., 2003. Developments in radiation, stimulation and observation facilities in luminescence measurements. Radiat. Meas. 37, 535–541.

Buylaert, J.P., Murray, A.S., Thomsen, K.J., Jain, M., 2009. Testing the potential of an elevated temperature IRSL signal from K-feldspar. Radiat. Meas. 44, 560–565.

Buylaert, J.-P., Jain, M., Murray, A.S., Thomsen, K.J., Thiel, C., Sobhati, R., 2012. A robust feldspar luminescence dating method for Middle and Late Pleistocene sediments. Boreas 41, 435–451.

Buylaert, J.-P., Murray, A.S., Gebhardt, A.C., Sobhati, R., Ohlendorf, C., Thiel, C., Wastegård, S., Zolitschka, B., The PASADO Science Team, 2013. Luminescence dating of the PASADO core 5022-1D from Laguna Potrok Aike (Argentina) using IRSL signals from feldspar. Quat. Sci. Rev. 71, 70–80.

Clarke, M.L., Rendell, H.M., 1997. Infra-red stimulated luminescence spectra of alkali feldspars. Radiat. Meas. 27, 221–236.

Colarossi, D., Duller, G.A.T., Roberts, H.M., Tooth, S., Lyons, R., 2015. Comparison of paired quartz OSL and feldspar post-IR IRSL dose distributions in poorly bleached fluvial sediments from South Africa. Quat. Geochronol. http://dx.doi.org/10.1016/j.quageo.2015.02.015 (in press).

Duller, G.A.T., 1992. Luminescence Chronology of Raised Marine Terraces South-west North Island New Zealand (Unpublished PhD thesis). University of Wales, Aberystwyth.

Duller, G.A.T., 2006. Single grain optical dating of glacigenic deposits. Quat. Geochronol. 1, 296–304.

Duller, G.A.T., 2008. Single-grain optical dating of Quaternary sediments: why aliquot size matters in luminescence dating. Boreas 37, 589–612.

Duller, G.A.T., Bøtter-Jensen, L., Murray, A.S., 2003. Combining infrared- and green-laser stimulation sources in single-grain luminescence measurements of feldspar and quartz. Radiat. Meas. 37, 543–550.

Godfrey-Smith, D.I., Huntley, D.J., Chen, W.-H., 1988. Optical dating studies of quartz and feldspar sediment extracts. Quat. Sci. Rev. 7, 373–380.
Guerin, G., Mercier, N., Adamiec, G., 2011. Dose-rate conversion factors: update. Anc. TL 29, 5–8.
Guerin, G., Mercier, N., Nathan, R., Adamiec, G., Lefrais, Y., 2012. On the use of the infinite matrix assumption and associated concepts: a critical review. Radiat. Meas. 47, 778–785.
Huntley, D.J., Lamothe, M., 2001. Ubiquity of anomalous fading in K-feldspars and the measurement and correction for it in optical dating. Can. J. Earth Sci. 38, 1093–1106.
Jain, M., Ankjærgaard, C., 2011. Towards a non-fading signal in feldspar: insight into charge transport and tunnelling from time-resolved optically stimulated luminescence. Radiat. Meas. 46, 292–309.
Kaplan, M.R., Strelin, J.A., Schaefer, J.M., Denton, G.H., Finkel, R.C., Schwartz, R., Putnam, A.E., Vandergoes, M.J., Goehring, B.M., Travis, S.G., 2011. In-situ cosmogenic ^{10}Be production rate at Lago Argentino, Patagonia: implications for late-glacial climate chronology. Earth Planet. Sci. Lett. 309, 21–32.
Kars, R.H., Reimann, T., Ankjærgaard, C., Wallinga, J., 2014. Bleaching of the post-IR IRSL signal: new insights for feldspar luminescence dating. Boreas 43, 780–791.
Li, B., Jacobs, Z., Roberts, R.G., Li, S.-H., 2014. Review and assessment of the potential of post-IR IRSL methods to circumvent the problem of anomalous fading in feldspar luminescence. Geochronometria 41, 178–201.
Madsen, A.T., Buylaert, J.-P., Murray, A.S., 2011. Luminescence dating of young coastal deposits from New Zealand using feldspar. Geochronometria 38, 378–390.
Murray, A.S., Thomsen, K.J., Masuda, N., Buylaert, J.P., Jain, M., 2012. Identifying well-bleached quartz using the differential bleaching rates of quartz and feldspar luminescence signals. Radiat. Meas. 47, 688–695.
Prescott, J.R., Hutton, J.T., 1994. Cosmic ray contributions to dose rates for luminescence and ESR dating: large depths and long-term time variations. Radiat. Meas. 23, 497–500.
Reimann, T., Tsukamoto, S., 2012. Dating the recent past (<500 years) by post-IR IRSL feldspar – examples from the North Sea and Baltic Sea coast. Quat. Geochronol. 10, 180–187.
Reimann, T., Tsukamoto, S., Naumann, M., Frechen, M., 2011. The potential of using K-rich feldspars for optical dating of young coastal sediments – a test case from Darss-Zingst peninsula (southern Baltic Sea coast). Quat. Geochronol. 6, 207–222.
Reimann, T., Thomsen, K.J., Jain, M., Murray, A.S., Frechen, M., 2012. Single-grain dating of young sediment using the pIRIR signal from feldspar. Quat. Geochronol. 11, 28–41.
Robertson, G.B., Prescott, J.R., Hutton, J.T., 1991. Bleaching of the thermoluminescence of feldspars by sunlight. Nucl. Tracks Radiat. Meas. 18, 101–107.
Smedley, R.K., 2014. Testing the Use of Single Grains of K-feldspar for Luminescence Dating of Proglacial Sediments in Patagonia (Unpublished Ph.D thesis). Aberystwyth University, U.K.
Smedley, R.K., Duller, G.A.T., 2013. Optimising the reproducibility of measurements of the post-IR IRSL signal from single-grains of feldspar for dating. Anc. TL 31, 49–58.
Smedley, R.K., Duller, G.A.T., Pearce, N.J., Roberts, H.M., 2012. Determining the K-content of single-grains of feldspar for luminescence dating. Radiat. Meas. 47, 790–796.
Sohbati, R., Murray, A.S., Buylaert, J.-P., Ortuño, M., Cunha, P.P., Masana, E., 2012. Luminescence dating of Pleistocene alluvial sediments affected by the Alhama de Murcia fault (eastern Betics, Spain) – a comparison between OSL, IRSL and post-IR IRSL ages. Boreas 41, 250–262.
Spooner, N.A., 1994. The anomalous fading of infrared-stimulated luminescence from feldspars. Radiat. Meas. 23, 625–632.
Thiel, C., Buylaert, J.-P., Murray, A., Elmejdoub, N., Jedoui, Y., 2012. A comparison of TT-OSL and post-IR IRSL dating of coastal deposits on Cap Bon peninsula, north-eastern Tunisia. Quat. Geochronol. 10, 209–217.
Thomsen, K.J., Murray, A.S., Bøtter-Jensen, L., 2005. Sources of variability in OSL dose measurements using single grains of quartz. Radiat. Meas. 39, 47–61.
Thomsen, K.J., Murray, A.S., Jain, M., Bøtter-Jensen, L., 2008. Laboratory fading rates of various luminescence signals from feldspar-rich sediment extracts. Radiat. Meas. 43, 1474–1486.
Thomsen, K.J., Murray, A.S., Jain, M., 2011. Stability of IRSL signals from sedimentary K-feldspar samples. Geochronometria 38, 1–13.
Trauerstein, M., Lowick, S., Pressuer, F., Rufer, D., Schlunegger, F., 2012. Exploring fading in single-grain feldspar IRSL measurements. Quat. Geochronol. 10, 327–333.
Vandergoes, M.J., Hogg, A.G., Lowe, D.J., Newnham, R.M., Denton, G.H., Southon, J., Barrell, D.J.A., Wilson, C.J.N., McGlone, M.S., Allan, A.S.R., Almond, P.C., Pletchey, F., Dabell, K., Dieffenbacher-Krall, A.C., Blaauw, M., 2013. A revised age for the Kawakawa/Oruanui tephra, a key marker for the Last Glacial Maximum in New Zealand. Quat. Sci. Rev. 74, 195–201.
Wallinga, J., Murray, A., Wintle, A., 2000. The single-aliquot regenerative-dose (SAR) protocol applied to coarse-grain feldspar. Radiat. Meas. 32, 529–533.
Zimmerman, D.W., 1971. Thermoluminescence dating using fine grains from pottery. Archaeometry 13, 29–52.